



## Degradation of dicamba – A persistent herbicide – By combined application of formic acid and UV as an advanced reduction process

Zahra Askarniya<sup>a,1</sup>, Łukasz Cichocki<sup>a,1</sup> , Sławomir Makowiec<sup>b</sup>, Chongqing Wang<sup>c</sup>, Grzegorz Boczkaj<sup>a,d,\*</sup> 

<sup>a</sup> Department of Sanitary Engineering, Faculty of Civil and Environmental Engineering, Gdansk University of Technology, G. Narutowicza St. 11/12, Gdansk 80 – 233, Poland

<sup>b</sup> Department of Organic Chemistry, Faculty of Chemistry, Gdansk University of Technology, G. Narutowicza St. 11/12, Gdansk 80 – 233, Poland

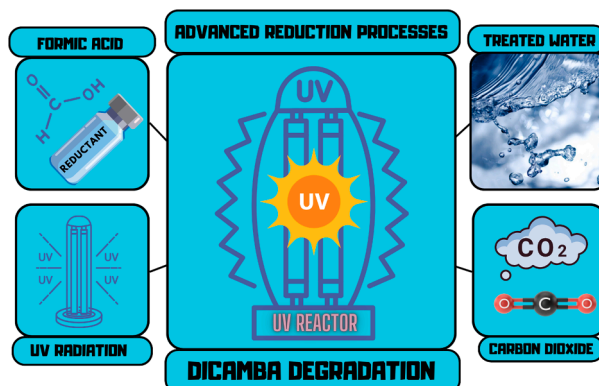
<sup>c</sup> School of Chemical Engineering, Zhengzhou University, Zhengzhou 450001, China

<sup>d</sup> School of Civil, Environmental, and Architectural Engineering, College of Engineering, Korea University, 145 Anam-ro, Seongbuk-gu, Seoul 02841, Republic of Korea

### HIGHLIGHTS

- Reductive removal of dicamba by the combination of UV and formic acid.
- Carboxyl anion radical as the main responsible for the dechlorination of dicamba.
- The superiority of ARP over photolysis by UV for the dechlorination of dicamba.
- Alternative ARP degradation mechanism comparing to existing AOPs.
- Easy applicability for industrial wastewater treatment plants.

### GRAPHICAL ABSTRACT



### ARTICLE INFO

#### Keywords:

Wastewater treatment  
Photolysis  
Emerging organic pollutants  
Effluents  
Hybrid processes

### ABSTRACT

The degradation of dicamba as a persistent herbicide was studied with the combined application of UV and formic acid (FA) as a novel advanced reduction process (ARP). The effects of key parameters of FA concentration, dissolved organic matter, and inorganic anions were studied. A 97 % degradation and 94 % dechlorination of dicamba were obtained through the combination of UV and FA (UV-FA) at a dicamba concentration of 0.023 mM and FA concentration of 0.123 M. With respect to the dechlorination, at a dicamba concentration of 0.23 mM, FA concentration of 0.123 M, and pH of 2, chloride concentration of 12.4 mg/L and 5.2 mg/L was obtained for ARP (UV-FA) and sole UV in acidic condition, respectively. Scavenging test using Methyl viologen ( $MV^{2+}$ ) as a scavenger for reductive radicals including carboxyl anion radicals ( $CO_2^{\cdot-}$ ) led to a decrease in the chloride concentration to 1.7 mg/L, revealing the importance of this radical in the dechlorination of dicamba. Inorganic

\* Correspondence to: Gdansk University of Technology, Faculty of Civil and Environmental Engineering, Department of Sanitary Engineering, G. Narutowicza St. 11/12, Gdansk 80 – 233, Poland.

E-mail addresses: [grzegorz.boczkaj@pg.edu.pl](mailto:grzegorz.boczkaj@pg.edu.pl), [grzegorz\\_boczkaj@korea.ac.kr](mailto:grzegorz_boczkaj@korea.ac.kr) (G. Boczkaj).

<sup>1</sup> Zahra Askarniya and Łukasz Cichocki have equally contributed to this work and mutually share the first co-authorship.

<https://doi.org/10.1016/j.jhazmat.2025.137984>

Received 19 August 2024; Received in revised form 14 March 2025; Accepted 15 March 2025

Available online 19 March 2025

0304-3894/© 2025 The Authors. Published by Elsevier B.V. This is an open access article under the CC BY license (<http://creativecommons.org/licenses/by/4.0/>).

anions ( $\text{CO}_3^{2-}$  and  $\text{SO}_4^{2-}$ ) had a slightly positive effect on the degradation of dicamba and led to an increase in degradation to 99 %, while they had a negative effect on the dechlorination by 7 % and 30 %, respectively. Due to the turbidity induced by dissolved organic matters (DOM), a moderate decrease in degradation by 39 % and dechlorination by 30 % was observed. The existence of five intermediates identified by GC-MS technique confirmed the proposed mechanism of dicamba degradation via ARP. Reductive degradation of dicamba mainly consists of processes based on  $\text{CO}_2^{\cdot-}$ , including single electron transfer process and radical-nucleophilic aromatic substitution (SRN) reactions, demonstrating the capability of this ARP for the effective degradation of dicamba.

## 1. Introduction

The excessive application of pesticides is one of the universal concern as these compounds can induce various environmental issues such as the contamination of soil and water [1,2]. Dicamba (2-methoxy-3,6-dichlorobenzoic acid) is a post-emergence herbicide that possesses an aromatic chlorinated structure with high stability. Dicamba mostly exists in its anionic state having high stability [3]. This herbicide inhibits the growth of undesired plants by interfering in their auxin hormone function and therefore, it is broadly applied for the control of broadleaf weeds [4]. Similar to all hydrophilic pesticides, dicamba can be easily released into the environment and cause widespread pollution through various ways such as rainwater and surface runoff [5]. It is also able to leach from soil, enter the groundwater, and as a result, pollute the ecosystems [6,7].

Chu and Wang [8] investigated the degradation of dicamba using the combination of  $\text{H}_2\text{O}_2$  and UV in the presence of  $\text{TiO}_2$  and reported that the addition of a catalyst accelerate the rate of degradation but they did not report the products of this oxidation. Chávez-Moreno et al. [9] performed research on the photo-catalytic ( $\text{TiO}_2$  anatase /UV 254 nm) degradation of dicamba and achieved 85 % degradation in 45 min, although, they did not discuss the products of this photocatalytic oxidation. Wan et al. [5] studied the removal of dicamba by the utilization of Biochar prepared from Fe-modified sludge and obtained a 92 % removal rate of this pollutant in 180 min, however, it was reported that the main products of this process were 3,6-dichlorosalicylic acid and 3,6-dichlorogentisic acid, and they were not able to achieve dechlorination of these secondary pollutants by this process. The removal of dicamba can be performed by anaerobic digestion, but this method is time-consuming. Liu et al. [10] reached 100 % removal of dicamba through anaerobic catabolism in 3 days. Gu et al. [11] achieved 100 % removal of dicamba using anaerobic microcosms under sulfate-reducing conditions enriched from sediment taken from a river as a source of microorganisms supplemented with yeast extract in 30 days. Yao et al. [12] investigated the removal of dicamba by the application of two sphingomonads and reported complete degradation of this compound in 36 h and 72 h.

Advanced reduction processes (ARPs) are an effective solution for the degradation of a variety of compounds and can provide effective alternatives to AOPs. There are a variety of AOPs widely investigated including catalyst-based AOPs [13,14], persulfate-based AOPs [15], and cavitation-based ones [16], which can generate various oxidizing radicals such as hydroxyl radicals ( $\cdot\text{OH}$ ) [17], sulfate radicals ( $\text{SO}_4^{\cdot-}$ ) [18], superoxide radicals ( $\text{O}_2^{\cdot-}$ ) [19], etc. These radicals can react with pollutant molecules leading to the oxidation of organic pollutants [19,20]. Alternatively, ARPs generate reductive radicals including hydrated electrons ( $e_{\text{aq}}^-$ ) [21], hydrogen radicals ( $\text{H}\cdot$ ) [22], sulfite radicals ( $\text{SO}_2^{\cdot-}$ ) [23], and carboxyl anion radicals ( $\text{CO}_2^{\cdot-}$ ) [24].

The effectiveness of ARPs is highly dependent on the molecular structure of pollutants [25]. Since the application of sole reductants is usually insufficient for efficient degradation, it is required to combine reductants with activation methods to generate the desired reductive radicals. UV light is one of those methods which are commonly utilized in ARPs [26]. Sulfite-based ARPs have drawn attention due to the generation of  $e_{\text{aq}}^-$  possessing a high reductive potential of (-2.3 V) and high resistance towards the negative effect of dissolved oxygen. On the other

hand, one important issue might be the generation of sulfur-containing by-products [27,28].

Carboxyl anion radical ( $\text{CO}_2^{\cdot-}$ ) is also a strong reductive radical with a reduction potential of  $-2.0$  V, which has high stability [29]. Although the reduction potential of  $\text{CO}_2^{\cdot-}$  is lower than the reduction potential of  $e_{\text{aq}}^-$ , it has attracted the attention of researchers due to its longer lifetime and easy generation [30]. This reductive radical can be generated as a result of a reaction between organic carboxylic acids such as formic acid and  $e_{\text{aq}}^-$ ,  $\text{H}\cdot$ , and  $\cdot\text{OH}$  [31]. This reductive radical can be utilized for the dehalogenation of toxic compounds. Liu et al. [24] have employed the combination of UV, titanium dioxide ( $\text{TiO}_2$ ), and formate to generate  $\text{CO}_2^{\cdot-}$  and reduce an aliphatic chlorinated disinfectant (trichloroacetic acid).

In this work, the degradation and dechlorination of dicamba as a persistent aromatic herbicide was studied using a combination of UV and formic acid as an ARP, and the results were compared with the results achieved by the sole use of UV in acidic conditions. In addition, the products of these processes were determined according to the results obtained by gas chromatography-mass spectrometry (GC-MS). The participation of reductive radicals in the degradation and dechlorination of dicamba was investigated using a scavenging test. Furthermore, the effect of a variety of factors such as the type of UV lamp, the concentration of formic acid, the effect of dissolved organic matter, as well as the effect of inorganic anions were studied.

## 2. Materials and methods

### 2.1. Chemicals

Formic acid 80 % (FA), acetonitrile (HPLC grade), dichloromethane (ACS), phosphoric acid (85 %), potassium iodide (pure) and acetone were purchased from POCH (Poland). Humic acid (97 %) was provided from Angene (China). Methyl viologen (98 % hydrate) was purchased from Thermo Scientific (Germany). Dicamba (97 %) was purchased from Biosynth (Slovakia). Sodium carbonate (99,9 %), sodium sulfate (99 %), and sulfuric acid (95 %) were provided by Chempur (Poland). Tert-butyl alcohol was purchased from STANLAB (Poland). All materials were of analytical grade and were utilized without further purification.

### 2.2. Procedure

A model solution of dicamba was prepared on a magnetic stirrer at room temperature. FA was added to the solution at the beginning of the experiments. The measurement of pH was performed by pH test strips (Merck, Germany). Experiments were carried out in two interconnected reactors (Figure S1). The first reactor was used for sample collection and cooling of the mixture. The second reactor was equipped with a UV mercury lamp (type UVQ 250Z, 250 W, UV-Technik, Germany) or a UV mercury-iron doped - lamp (type UVH-F, 250 W, UV-Technik, Germany). The total volume of connected reactors was 7.5 L. The temperature in the reaction system was maintained at 20 °C, and the system was hermetically sealed throughout the process. The mixture was circulated between the reactors using a model 505 L peristaltic pump (Watson Marlow, UK) with a speed of 220 RPM (flow rate of 1.3 L/min). The total treatment time for all experiments was 240 min and samples were taken every 60 min. Initial samples were taken before the addition

of FA.

Deionized water (Direct-Q® Water Purification System – Merck Millipore) was used in all of the experiments. A dicamba concentration of 0.023 mM (5 ppm) was used for most of the experiments. However, for scavenging tests as well as the tests performed for the comparison between UV-FA and sole UV, the initial concentration of dicamba was 10 times higher (0.23 mM) to observe the differences more obviously.

For the determination of the reductive radicals, the scavenging test was performed using methyl viologen and tert-butyl alcohol as scavengers. Humic acid was also added to the solution to investigate the effect of DOM on degradation and dechlorination. The effect of inorganic anions was studied with the addition of inorganic anions at a molar ratio of anions to the pollutant of 100:1. The degradation % was calculated by Eq. 1.

$$\text{Degradation\%} = \frac{C_0 - C}{C_0} \times 100 \quad (1)$$

Where  $C_0$  and  $C$  represent the initial concentration of dicamba and the concentration of dicamba at time  $t$ , respectively.

### 2.3. Kinetic study

The degradation kinetics of dicamba were analyzed, and the pseudo first-order rate constant ( $k_1$ ) and pseudo second-order rate constant ( $k_2$ ) were calculated through following Eqs [32]:

$$\frac{dC}{dt} = -k_1 C \quad (2)$$

$$\ln\left(\frac{C_0}{C}\right) = k_1 t \quad (3)$$

$$\frac{dC}{dt} = -k_2 C^2 \quad (4)$$

$$\frac{1}{C} - \frac{1}{C_0} = k_2 t \quad (5)$$

Where  $k_1$ ,  $k_2$ ,  $C_0$ ,  $t$ , and  $C$  represent first-order degradation rate constant, second-order degradation rate constant, the initial concentration of dicamba, time of process, and the concentration of dicamba at time  $t$ , respectively.

### 2.4. Quantitative analysis

Determination of the concentration of dicamba was accomplished by the application of high-performance liquid chromatography (HPLC) consisting of a chromatograph (model: LaChrome, MERCK-HITACHI, Germany), an interface (model D-7000, MERCK-HITACHI, Germany), a pump (model L-7100, MERCK-HITACHI, Germany), an injector (model: Rheodyne 7125, IDEX Health & Science, LLC, USA), a chromatographic column (model: Zorbax C-18, 3.5  $\mu\text{m}$ , 4.6  $\times$  150 mm, Agilent, USA), and a UV-VIS detector (model: L-7420, MERCK-HITACHI, Germany). The mobile phase was a mixture of acetonitrile and deionized water at a pH of 3 adjusted by sulfuric acid. The ratio of acetonitrile: water was 50:50. Isocratic conditions with a flow rate of 1.0 mL  $\text{min}^{-1}$  were applied. The detection wavelength of the UV-VIS detector was 210 nm.

A chloride anions concentration in the samples was determined using a mercuric thiocyanate method for the determination of chlorides provided by HACH tests and a spectrophotometer HACH DR/2010.

The by-product analysis was performed using a gas chromatograph (model GC-2010 Plus, Shimadzu, Japan) coupled with a mass spectrometer (model GCMS-QP2010 SE, Shimadzu, Japan). Samples for analysis were prepared using a dispersive liquid-liquid microextraction (DLLME). A 0.9 mL of the mixture of dispersing and extraction solvent composed of acetone (0.4 mL) and dichloromethane (0.5 mL) was used

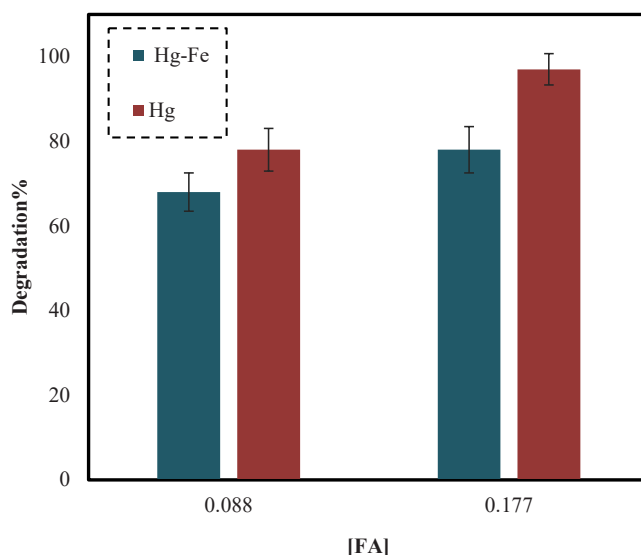


Fig. 1. Degradation achieved by two different UV lamps at a [dicamba]: 0.023 mM, [FA]: 0.088 M and 0.177 M.

for by-product extraction. The extraction was carried out by shaking 5 mL of sample with 0.9 mL of extraction mixture for 1 minute. Next, the samples were centrifuged for 10 min at 5000 rpm (EBA 8S, Hettich, Germany). A 0.3 mL of dichloromethane phase was taken from the vials by automatic micropipette and placed in autosampler vials equipped with glass conical micro-inserts for GC-MS analysis. The separation conditions were as follows: a capillary column RTX®-100-DHA (100 m  $\times$  0.25 mm ID  $\times$  0.5  $\mu\text{m}$  df), carrier gas was hydrogen at 1 mL/min, injection port temperature was 250  $^{\circ}\text{C}$ . Samples were injected by auto-sampler (injection volume 1  $\mu\text{L}$ , splitless mode). Samples were separated under temperature programming conditions at an initial temperature of 35  $^{\circ}\text{C}$  for 5 min, followed by a temperature ramp at 15  $^{\circ}\text{C}/\text{min}$ , up to 250  $^{\circ}\text{C}$ , followed by isothermal separation at 250  $^{\circ}\text{C}$  for 20 min. The mass spectrometer interface temperature was 250  $^{\circ}\text{C}$ , while the ion source temperature was 200  $^{\circ}\text{C}$ . MS was operated at scan mode (range from 34  $m/z$  to 350  $m/z$ ).

Spectrophotometric analysis of potassium iodide solution was carried out on a spectrophotometer (UV-1900i, Shimadzu, Japan) for wavelength 352 nm to confirm the presence of hydroxyl radicals under mercury UV lamp (used in current study) irradiation of water.

## 3. Result and discussion

The degradation of dicamba was investigated using the combined process of FA-UV and the effects of a variety of parameters have been studied to determine the most effective conditions. The results of this investigation have been discussed in the following paragraphs.

### 3.1. Effect of UV lamp type

In this study, two different UV lamps: a UV mercury doped with iron lamp (emission spectrum provided in Figure S2) and a UV mercury lamp (emission spectrum provided in Figure S3). The following reactions can occur when the solution of formic acid is exposed to UV irradiation [24, 33].



The characteristics of a UV lamp determine its effectiveness for the

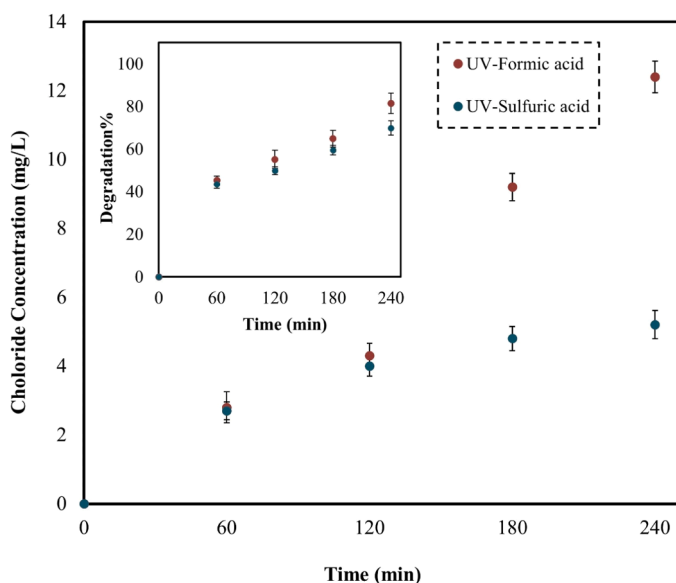


Fig. 2. Comparison between UV-Formic acid and UV-Sulfuric acid processes ([dicamba]: 0.23 mM, [FA]: 0.123 M, pH: 2).

dissociation of  $H_2O$  and the generation of  $\cdot OH$  and  $H\cdot$  which consequently leads to the generation of reductive  $CO_2^{\cdot -}$ . Two different UV lamps were employed at two constant concentrations of formic acid (0.088 M and 0.177 M) to select the most effective one in this combined process. The experiments were performed at a dicamba concentration of 0.023 mM, and the results are demonstrated in Fig. 1.

As it is obvious from Fig. 1, the UV mercury lamp was more effective for the dissociation of  $H_2O$  leading to the generation of reactive radicals, hence, the rest of experiments were performed using this lamp. Based on the spectrum of the mercury lamp (Figure S3), it can be seen that most of the UV energy is generated in the wavelength range of 200–320 nm, while in the case of the iron-doped mercury lamp (Figure S2), this range is extended from 200 to 450 nm. Such results, considering the same lamp power values, indicate that the optimum wavelength for the absorbance and dissociation of  $H_2O$  to radicals is in the range of 200–320 nm, which is in agreement with the research proving that UVC spectral range is capable for UV photolysis of water, as water absorb photons and can generate hydroxyl radicals upon photon absorption [34].

Additionally, to identify the generation of hydroxyl radicals as a result of the irradiation by mercury UV lamp used during the experiment, a solution of 5 mM potassium iodide (KI) was used and exposed to UV irradiation for 60 min. The following reactions can happen at the presence of  $\cdot OH$  and KI [35,36]:



The effects of oxidation of I<sup>-</sup> (Eq. 9) by hydroxyl radicals were visible by changing the color of the solution from transparent at the beginning to yellow at the end of the experiment. The samples were then analyzed in a spectrophotometer - monitored wavelength was 352 nm. The linear increase of iodine in the sample was a clear proof of  $\cdot OH$  generation through UV radiation [35], which can react with FA to generate  $CO_2^{\cdot -}$  in the main experiments.

Table 1

Kinetic study for the degradation achieved by UV-Formic acid and UV-Sulfuric acid processes ([dicamba]: 0.23 mM, [FA]: 0.123 M, pH: 2).

Process	First-order rate constant		Second-order rate constant	
	R <sup>2</sup>	k <sub>1</sub> (min <sup>-1</sup> )	R <sup>2</sup>	k <sub>2</sub> (M <sup>-1</sup> min <sup>-1</sup> )
UV-Formic acid	0.952	0.0067	0.848	0.0003
UV-Sulfuric acid	0.906	0.0053	0.964	0.0002

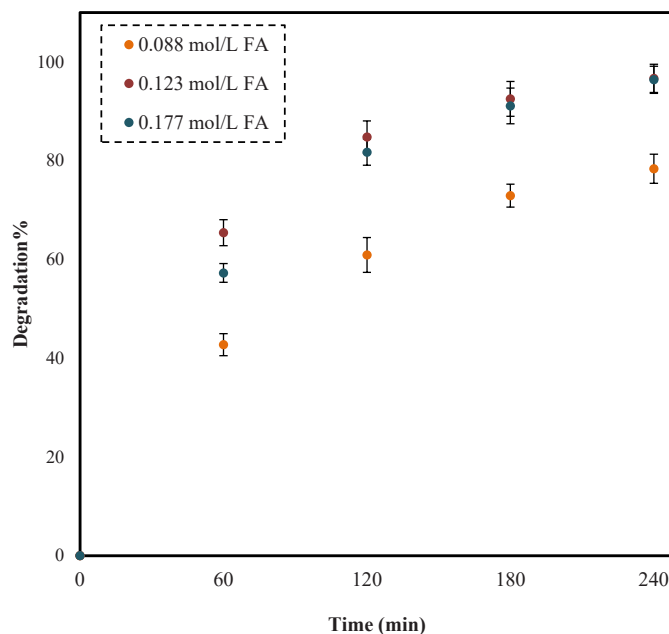


Fig. 3. Effect of FA concentrations on the degradation of dicamba ([dicamba]: 0.023 mM, pH: 2).

### 3.2. Comparison of combined processes of UV-FA and sole UV

To determine the superiority of the reduction process done by  $CO_2^{\cdot -}$  (reduction potential of  $-2.0$  V) formed under the combined application of UV and FA over sole UV which can decompose the dicamba directly by photolysis or indirectly by the generated  $\cdot OH$  (oxidation potential of 2.8 V) according to Eq. 6, the degradation and dechlorination achieved by these two processes were compared. Sulfuric acid was used instead of FA to adjust the initial pH in the sole UV process. In this experiment, higher concentration of dicamba (0.23 mM) was applied to observe the level of dechlorination more accurately, and the difference between sole UV and UV-FA as an ARP more obviously. The results are presented in Fig. 2.

As it is observed in Fig. 2, sole UV resulted in 70 % degradation while the ARP by the combination of FA and UV led to 82 % degradation in 240 min. A more obvious difference was observed in relation to changes in chloride concentration. In the case of ARP, intensification in dechlorination reactions was expected. The chloride concentration observed in the combination of FA and UV was 12.4 mg/L, while in the case of sulfuric acid and UV the chloride concentration was just 5.2 mg/L in 240 min. Thus, in both aspects, ARP-based treatment revealed superiority compared to sole UV. The kinetic results are reported in Table 1. According to coefficients of determination (R<sup>2</sup>) reported in the table, the first-order rate constants are acceptable in these two experiments. The first-order rate constant obtained in the reduction process by means of UV and FA was 0.0067 min<sup>-1</sup>, while the first-order rate constant achieved by sole UV in acidic conditions adjusted by sulfuric acid was 0.0053 min<sup>-1</sup>.

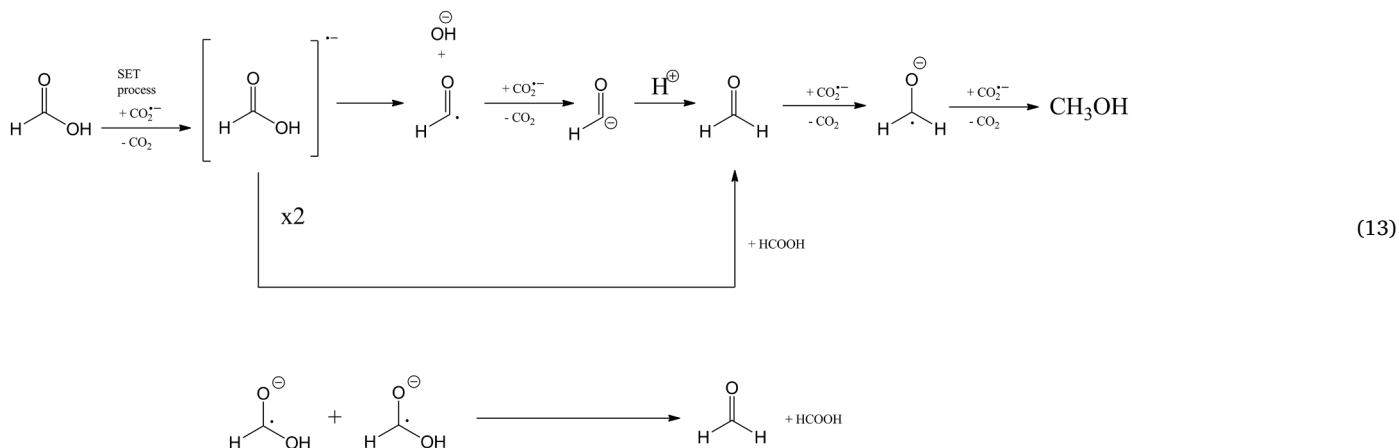
The differences observed in these two processes can be due to the reason that ARPs can be more effective in the case of degradation of

halogenated compounds. Furthermore,  $\text{CO}_2^{\bullet-}$  is highly stable and possesses a long lifetime, while  $\bullet\text{OH}$  has a short lifetime, which can be another reason for the lower degradation observed by sole UV [24]. According to the dechlorination results, the ARP done by the combined process of FA and UV had the potential of dehalogenation while sole UV in acidic conditions was not as capable as the ARP [37]. It can be attributed to the fact that the oxidative breakage of the Cl-C bond requires a higher oxidative potential than 2 V, while the reductive breakage can be obtained more easily [24,26].

### 3.3. Effect of formic acid concentration

FA concentration can have an important impact on the efficiency of degradation by FA under UV irradiation conditions. As demonstrated in Fig. 3, an increase in FA concentration from 0.088 M to 0.123 M resulted in an increase in the degradation of dicamba from 87 % to 97 % in 240 min.

Further increase showed a small decrease in degradation rate, which was attributed to the self-scavenging effect of excessive radicals formed at higher concentrations of formic acid (Eq. 13) [38].



The kinetic data are demonstrated in Table 2, and again first-order rate constants are valid.

Accordingly, an increase in the concentration of FA up to a maximum amount of 0.123 M increased the first-order rate constant from  $0.0069 \text{ min}^{-1}$  to  $0.0146 \text{ min}^{-1}$ . Further increase in this parameter till 0.177 M had a negligible effect on the degradation and decreased it to  $0.0140 \text{ min}^{-1}$ . The ascending trend can be related to the fact that an increase in the concentration of FA as a reactant can lead to an increase in the formation of  $\text{CO}_2^{\bullet-}$  which can be one of the most important radicals in the degradation of dicamba via the combination of UV and FA. However,  $\bullet\text{OH}$  can also have the potential to oxidize this herbicide.

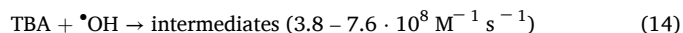
**Table 2**

Kinetic study for the degradation achieved by UV-Formic acid at different concentration of FA ([dicamba]: 0.023 mM, pH: 2).

Process	First-order rate constant		Second-order rate constant	
	R <sup>2</sup>	k <sub>1</sub> (min <sup>-1</sup> )	R <sup>2</sup>	k <sub>2</sub> (M <sup>-1</sup> min <sup>-1</sup> )
[FA]: 0.088 M	0.965	0.0069	0.991	0.0029
[FA]: 0.123 M	0.991	0.0146	0.801	0.0186
[FA]: 0.177 M	0.998	0.0140	0.738	0.0175

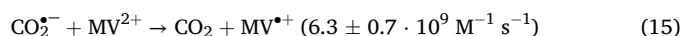
### 3.4. Identification of radical species

While the identification of  $\bullet\text{OH}$  was carried out using potassium iodide and subsequent analysis of samples in a spectrophotometer, to verify the importance of  $\bullet\text{OH}$ , which can react with FA and generated reductive  $\text{CO}_2^{\bullet-}$ , tert-butyl alcohol (TBA) was used as a scavenger for this radical according to Eq. 14 [39].



This experiment was conducted at a [FA] of 0.123 M, [dicamba] of 0.23 mM, and FA: TBA of 1:10.

The role of reductive  $\text{CO}_2^{\bullet-}$  in the degradation and dechlorination of dicamba was determined by performing a radical quenching test, applying Methyl viologen ( $\text{MV}^{2+}$ ) as a scavenger which consumes this radical and generate  $\text{CO}_2$  according to Eq. 15 [40]:



For this purpose, the experiment was accomplished at a [FA] of 0.123 M, [dicamba] of 0.23 mM, and  $[\text{MV}^{2+}]$  of 0.39 Mm.

The results of scavenging tests were illustrated in Fig. 4.

As observed in Fig. 4, TBA has decreased both degradation (from 82 % to 57 %) and dechlorination (from 12.4 to 5.6 mg/L). The presence of TBA might have hindered the generation of reductive  $\text{CO}_2^{\bullet-}$  due to the consumption of  $\bullet\text{OH}$ , however, this reductive radical could be still generated through a reaction between FA and  $\text{H}^{\bullet}$  (Eq. 8).

The presence of  $\text{MV}^{2+}$  resulted in an obvious decrease in the degradation of dicamba from 82 % to 55 % in 240 min. Furthermore, it drastically decreased the concentration of chloride from 12.4 to 1.7 mg/L (84 % reduction), revealing the significant role of reduction performed by  $\text{CO}_2^{\bullet-}$  in the dechlorination of dicamba. Further discussion and proofs of  $\text{CO}_2^{\bullet-}$  role in the degradation process are provided in Par. 3.7 (degradation mechanism). The kinetic results are reported in Table 3.

As observed, the first-order rate constant decreased from  $0.0067 \text{ min}^{-1}$  to  $0.0036 \text{ min}^{-1}$  and  $0.0034 \text{ min}^{-1}$  due to the presence of TBA and  $\text{MV}^{2+}$ , respectively. According to the results, the reductive radicals including  $\text{CO}_2^{\bullet-}$  had a contribution to the degradation especially in the dehalogenation of dicamba.

### 3.5. Effect of inorganic anions

Various dissolved compounds including inorganic anions are present in natural water. The quality of water can have a significant impact on

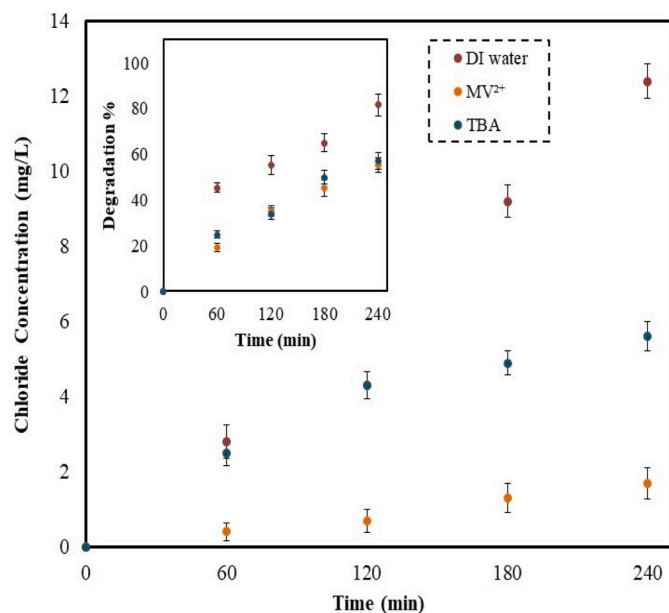


Fig. 4. Degradation and dechlorination achieved in the scavenging test ([dicamba]: 0.23 mM, [FA]: 0.123 M).

Table 3

Kinetic study for the degradation achieved by UV-FA in the presence of the scavenger ([dicamba]: 0.23 mM, [FA]: 0.123 M).

Process	First-order rate constant		Second-order rate constant	
	R <sup>2</sup>	k <sub>1</sub> (min <sup>-1</sup> )	R <sup>2</sup>	k <sub>2</sub> (M <sup>-1</sup> min <sup>-1</sup> )
UV-FA	0.952	0.0067	0.848	0.0003
UV-FA-TBA	0.984	0.0036	0.982	0.0001
UV-FA-MV <sup>2+</sup>	0.997	0.0034	0.988	0.0001

the effectiveness of applied treatment methods; therefore, it is important to study the influence of common anions found in natural water on the degradation of contaminations. For this aim, experiments were done in the presence of Na<sub>2</sub>SO<sub>4</sub> and Na<sub>2</sub>CO<sub>3</sub> at a ratio of 100 ( $\frac{Anion}{Dicamba} = 100$ ), a dicamba concentration of 0.023 mM, and FA concentration 0.123 M in 240 min, and the results are demonstrated in Fig. 5.

As shown, the presence of both inorganic anions slightly increased the degradation of dicamba and more obviously, the first-order rate constant of the process (Table 4). Nevertheless, CO<sub>3</sub><sup>2-</sup> slightly and SO<sub>4</sub><sup>2-</sup> obviously led to a decline in dechlorination.

The presence of CO<sub>3</sub><sup>2-</sup> increased the degradation and first-order rate constant from 97 % and 0.0146 min<sup>-1</sup> to 99 % and 0.0198 min<sup>-1</sup>, respectively. CO<sub>3</sub><sup>2-</sup> can react with •OH generated by UV and lead to the production of CO<sub>3</sub><sup>•-</sup> at a second-order rate constant of  $3.9 \times 10^8$  M<sup>-1</sup>s<sup>-1</sup> according to Eq. 16 [41].



Although CO<sub>3</sub><sup>•-</sup> possesses lower oxidation potential (1.59 V) compared to •OH (2.8 V), it has higher selectivity and longer lifetime, which can be the reason for its better performance in the degradation of some pollutants [19,42,43]. However, the existence of CO<sub>3</sub><sup>•-</sup> in the solution caused a reduction in the concentration of chloride from 1.5 mg/L to 1.4 mg/L. This decrease in the concentration of chloride can be attributed to the fact that CO<sub>3</sub><sup>•-</sup> consumed •OH which was utilized for the generation of reductive CO<sub>2</sub><sup>•-</sup> according to Eqs. 7 and 8, and

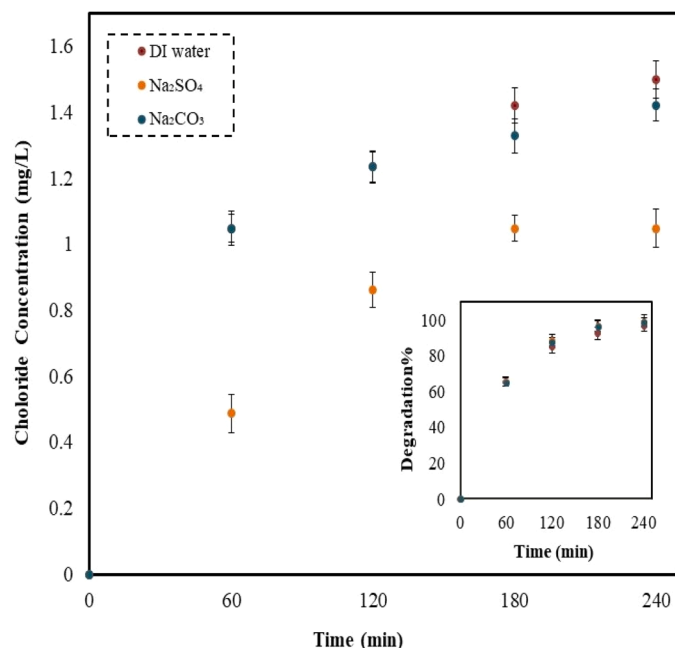


Fig. 5. Effect of inorganic anions on the degradation and dechlorination ([dicamba]: 0.023 mM, [FA]: 0.123 M,  $\frac{Anion}{Dicamba} = 100$ ).

Table 4

Kinetic study for the degradation achieved by UV-FA in presence of inorganic anions ([dicamba]: 0.023 mM, [FA]: 0.123 M,  $\frac{Anion}{Dicamba} = 100$ ).

Process	First-order rate constant		Second-order rate constant	
	R <sup>2</sup>	k <sub>1</sub> (min <sup>-1</sup> )	R <sup>2</sup>	k <sub>2</sub> (M <sup>-1</sup> min <sup>-1</sup> )
UV-FA-CO <sub>3</sub> <sup>2-</sup>	0.995	0.0198	0.671	0.0464
UV-FA-SO <sub>4</sub> <sup>2-</sup>	0.994	0.0192	0.613	0.0726

consequently, led to a reduction in the concentration of this reductive radical. As proved by scavenging tests, this radical had the primary role in the dechlorination of dicamba.

The presence of SO<sub>4</sub><sup>2-</sup> resulted in an increase in degradation and first-order rate constant from 97 % and 0.0146 min<sup>-1</sup> to 99 % and 0.0192 min<sup>-1</sup>, respectively. SO<sub>4</sub><sup>2-</sup> can react with •OH and generate SO<sub>4</sub><sup>•-</sup> at a second-order rate constant of  $6.5 \times 10^7$  M<sup>-1</sup>s<sup>-1</sup> according to Eq. 17 [44].



An increase observed for the degradation of the herbicide and the first-order rate constant of the reaction can be related to the fact that SO<sub>4</sub><sup>•-</sup> has similar or even higher redox potential (2.5–3.1 V) than •OH and has higher stability. Hence, it can react with dicamba and lead to its oxidation [45,46]. While •OH reacts non-selectively, SO<sub>4</sub><sup>•-</sup> is a selective radical that preferably reacts with electron-donating groups including hydroxyl (-OH), alkoxy (-OR), and  $\pi$  electrons of aromatic compounds in dicamba molecules [47].

Nevertheless, the presence of this anion had made an obvious decrease in chloride concentration from 1.5 mg/L to 1.05 mg/L. This descending trend can result from the consumption of •OH used for initiating the production of reductive CO<sub>2</sub><sup>•-</sup> which is the main responsible for the dechlorination of dicamba.

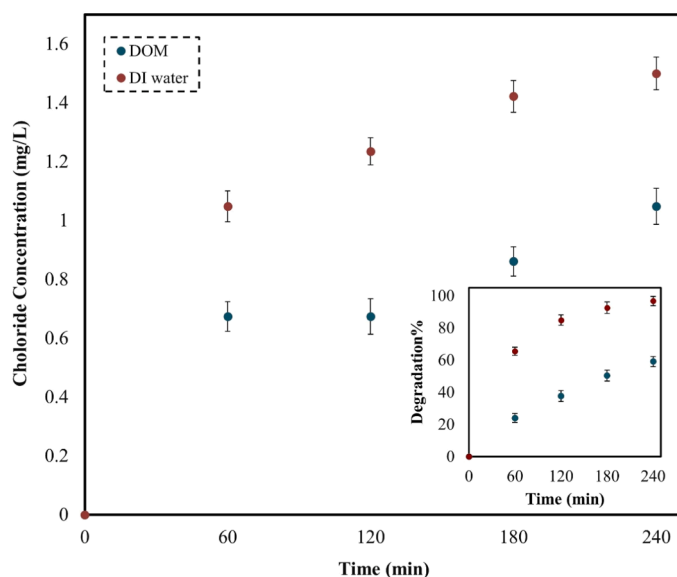


Fig. 6. Effect of DOM on the degradation and dechlorination ([dicamba]: 0.023 mM, [FA]: 0.123 M).

Table 5

Kinetic study for the degradation achieved by UV-FA in the presence of dissolved organic matter (DOM) ([dicamba]: 0.023 mM, [FA]: 0.123 M).

Process	First-order rate constant		Second-order rate constant	
	R <sup>2</sup>	k <sub>1</sub> (min <sup>-1</sup> )	R <sup>2</sup>	k <sub>2</sub> (M <sup>-1</sup> min <sup>-1</sup> )
UV-FA	0.991	0.0146	0.801	0.0186
UV-FA-DOM	0.994	0.0038	0.990	0.0011

### 3.6. Effect of dissolved organic matter

Wastewater usually contains dissolved organic matter (DOM) which can have a great influence on the efficiency of pollutant degradation [24]. Therefore, the effect of this factor on the degradation and dechlorination of dicamba using the combination of UV and FA at a dicamba concentration of 0.023 mM, FA concentration of 0.123 M, and humic acids concentration of 100 mg/L was investigated. In the literature, humic acids are commonly used to study the effect of DOM on effectiveness of the treatment process. Humic acids contain two fractions: humin (insoluble in water, which are often particles suspended in solution and significantly affect the transparency of the solution) and fulvic acids (easily soluble in water, which are precisely the DOM fraction). The results are demonstrated in Fig. 6.

The presence of humic acid in the solution has caused a significant decrease in the degradation of dicamba from 97 % to 59 %. It has led to a reduction in dechlorination from 1.5 mg/L to 1.05 mg/L. This descending trend can be attributed to the turbidity induced by humic acid in the solution which can cause a reduction in the effectiveness of the UV lamp leading to a decrease in the number of reactive radicals responsible for the degradation and dechlorination. However, in an industrial scale, filtration before the treatment can be suggested as a solution for this issue since it can decrease the level of turbidity by removing the water-insoluble fraction of humin. The kinetic results are reported in Table 5.

The adverse effect of dissolved organic matter is more obvious on the first-order rate constant. The first-order rate constant has significantly decreased from 0.0146 min<sup>-1</sup> to 0.0038 min<sup>-1</sup> as the result of the presence of humic acid regarded as the dissolved organic matter.

### 3.7. Degradation mechanism and by-products identification

After the analysis of the obtained results from GC-MS, the hypothesis regarding the degradation of dicamba has been discussed in the following paragraph. The existence of five compounds shown in the black frame (No. 4, 6, 8, 10, and 12) was confirmed by MS spectrometry.

As it is observed in Fig. 7, the reaction mechanism which assumes the following phenomena was proposed: reductive degradation of dicamba mainly consists of two processes, which both are related to the activity of carbon dioxide radical anion (CO<sub>2</sub><sup>•-</sup>). The first single electron transfer process (SET) leads to the formation of a radical anion (2), which can undergo two parallel processes, first with leaving the protonated carboxyl group as formic acid leading to the formation of radical (3). Radical (3) is again reduced by CO<sub>2</sub><sup>•-</sup>. Steric hindrance of radical (3) with two ortho substituents forbids any other possibility of reaction in such a case. Anion resulted from the reduction is protonated and product (4) is formed. However, further transformations of compound (4) are also possible, especially, the formation of compounds (6), (8), and (10), which were observed from GC-MS chromatograms. The following reaction mechanism was proposed: compound (4) is reduced with CO<sub>2</sub><sup>•-</sup> and then, the loss of methanol or chlorine anion may occur leading to the formation of radicals (5) or (7). Since radicals (5) or (7) are not sterically hindered, S<sub>RN</sub> process [48–50] is possible with CO<sub>2</sub><sup>•-</sup> as the best nucleophilic species in the reaction mixture. Following two SET processes formylxy derivative is formed which may hydrolyze in the solution leading to the formation of compound (6) or (8), a similar process is responsible for the formation of compound (10). As it was mentioned, compound (2) has also an alternate way of decomposition, and it consists of a similar process as described before: compound (2) decomposes into radical (11) and chlorine anion. Unhindered radical (11) may undergo S<sub>RN</sub> process as described before. Thus, 6-chloro-3-(formylxy)-2-methoxybenzoic acid (12) is formed, which was directly observed on GC-MS chromatograms.

At the end, a comparison was made between the results achieved in this study and the results reported in the literature. This comparison is observed in Table 6.

As it is observed, in most cases, the degradation of dicamba was just reported and there was no data about dechlorination. Complete degradation of dicamba was reported in most processes. The time of processes varies from 30 min to 720 h. The highest dechlorination (100 %) was obtained through UV+TiO<sub>2</sub> in 90 min. The lowest degradation (84 %) reported through Fe<sup>0</sup> + Al<sub>2</sub>(SO<sub>4</sub>)<sub>3</sub>, which was one of the slowest processes (156 h). In case of the fastest process (20 min) based on biomass tar-derived foams, the removal was obtained by adsorption not degradation. The slowest process (30 days) was anaerobic microcosms under sulfate-reducing conditions supplemented with yeast extract, respectively. It can be concluded that currently developed approach provide comparable effectiveness to the best available processes, but with different (ARP-based) mechanism of degradation. Advantage of current ARP process rely on process simplicity. There is no need to add photocatalyst (TiO<sub>2</sub>, [54]), omitting the need of its removal from post-process effluent, recycling and final disposal. While, application of homogeneous –photo Fenton based process ([56]) demands addition of iron ion into the effluents changing its composition and also could cause issues in real case scenario related to sludge formation.

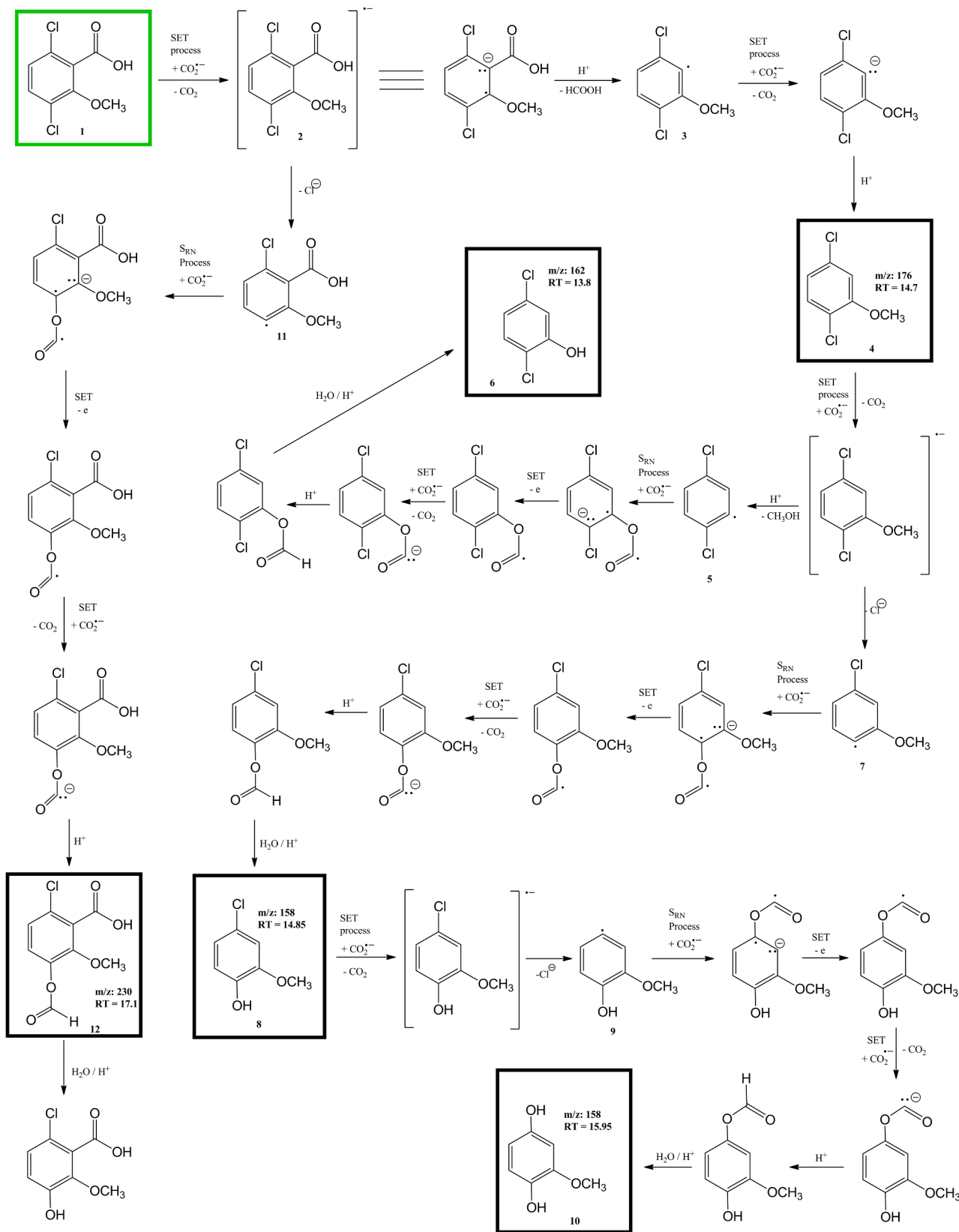


Fig. 7. Mechanism of dicamba degradation in the ARP/HCOOH/UV process.



**Table 6**

Comparison made in degradation and dechlorination between this study and literature.

Process	Time (h)	Degradation %	Dechlorination %	Ref.
<i>This study (UV-FA)</i>	4	97	94	
Hydrochar-montmorillonite composite/ peroxymonosulfate	4.2	100	n.s.*	[51]
TiO <sub>2</sub> +UV	0.75	85	n.s.	[9]
Biochar prepared from Fe-modified sludge	3	92.1	n.s.	[5]
Anaerobic sludge acclimated from river sediment	72	100	n.s.	[10]
Sphingobium sp. Ndbn-10	36	100	n.s.	[12]
Sphingomonas sp. Ndbn-20	72	100	n.s.	[11]
Anaerobic microcosms under sulfate-reducing condition supplemented with yeast extract	720	100	n.s.	[11]
Fe <sup>0</sup> + Al <sub>2</sub> (SO <sub>4</sub> ) <sub>3</sub>	156	84	96	[52]
Zero-valent iron powder	0.7	100	n.s.	[53]
UV+TiO <sub>2</sub>	1.5	100	100	[54]
Biomass tar-derived foams (adsorptive removal)	0.3	98	n.s.	[55]
Catalytic photo-Fenton (Fe(III)/H <sub>2</sub> O <sub>2</sub> /UV)	2	100	98.2	[56]

\* n.s. – not studied.

#### 4. Conclusion

Dicamba was effectively degraded by the utilization of the hybrid process of UV-FA. A degradation of 97 % ( $k = 0.0146 \text{ min}^{-1}$ ) and dechlorination of 94 % ( $1.5 \text{ mg L}^{-1}$  chloride concentration) were achieved at an optimum FA concentration of 0.123 M for dicamba concentration of 0.023 mM in 240 min process time. To compare the effectiveness of the ARP (UV-FA) with sole UV (UV-SA), higher concentration of dicamba (0.23 mM) was used and 82 % degradation and  $12.4 \text{ mg L}^{-1}$  chloride concentration were obtained by UV-FA, while just 70 % degradation and  $5.2 \text{ mg L}^{-1}$  chloride concentration were observed by UV-SA, demonstrating the important role of reductive agent in the dechlorination of dicamba. The  $\text{CO}_2^-$  were the reductive species which had a significant participation in the degradation and especially in the dechlorination of dicamba, confirmed by the addition of methyl viologen into the solution as the scavenging test. An increase in FA till an optimum value of 0.123 M enhanced the degradation of dicamba, and further increase slightly decreased the degradation. The presence of humic acid as a dissolved organic matter lowered the degradation and dechlorination effectiveness.  $\text{CO}_3^{2-}$  and  $\text{SO}_4^{2-}$  were used to investigate the effect of the water matrix and it was observed that they slightly increased the degradation. In the end, the formation of five products was confirmed by mass spectrometry, providing insight into the degradation mechanism. Developed process has high applicability in real-case scenario, due to high effectiveness in the presence of anions as well as effective dechlorination of the treated pollutant.

#### Environmental implications

This paper presents a novel process for target application in wastewater treatment. The degradation and dechlorination of dicamba as a persistent aromatic herbicide was studied using a combination of UV and formic acid as an ARP generating carboxyl anion radical ( $\text{CO}_2^{\bullet-}$ ), and the results were compared with the results achieved by the sole use of UV in acidic conditions. The products of these processes were also determined according to the results obtained by gas chromatography-mass spectrometry (GC-MS). This research paper presents extensive results, which are important in further understanding of advanced reduction processes for the dehalogenation of persistent compounds.

#### CRedit authorship contribution statement

**Cichocki Łukasz:** Writing – original draft, Visualization, Investigation, Data curation, Conceptualization. **Askarniya Zahra:** Writing – original draft, Visualization, Investigation, Data curation, Conceptualization. **Wang Chongqing:** Writing – review & editing, Validation, Formal analysis. **Makowiec Sławomir:** Writing – review & editing, Validation, Investigation, Data curation. **Boczkaj Grzegorz:** Writing – review & editing, Writing – original draft, Validation, Supervision, Resources, Project administration, Methodology, Funding acquisition, Formal analysis, Conceptualization.

#### Declaration of Competing Interest

The authors declare that they have no known competing financial interests or personal relationships that could have appeared to influence the work reported in this paper.

#### Acknowledgement

The authors gratefully acknowledge financial support from the National Science Centre, Warsaw, Poland for project OPUS nr UMO-2021/41/B/ST8/0157.

#### Appendix A. Supporting information

Supplementary data associated with this article can be found in the online version at [doi:10.1016/j.jhazmat.2025.137984](https://doi.org/10.1016/j.jhazmat.2025.137984).

#### Data availability

No data was used for the research described in the article.

#### References

- Niemi, R.M., et al., 2009. Microbial toxicity and impacts on soil enzyme activities of pesticides used in potato cultivation. *Appl Soil Ecol* 41 (3), 293–304.
- Morillo, E., Villaverde, J., 2017. Advanced technologies for the remediation of pesticide-contaminated soils. *Sci Total Environ* 586, 576–597.
- Milligan, P.W., Häggblom, M.M., 1999. Biodegradation and biotransformation of dicamba under different reducing conditions. *Environ Sci Technol* 33 (8), 1224–1229.
- Herman, P.L., et al., 2005. A three-component dicamba O-demethylase from *Pseudomonas maltophilia*, strain DL-6: gene isolation, characterization, and heterologous expression. *J Biol Chem* 280 (26), 24759–24767.
- Wan, C., et al., 2021. Mechanism of removal and degradation characteristics of dicamba by biochar prepared from Fe-modified sludge. *J Environ Manag* 299, 113602.
- Pavel, E.W., et al., 1999. Anaerobic degradation of dicamba and metribuzin in riparian wetland soils. *Water Res* 33 (1), 87–94.
- Zhao, H., Jaynes, W.F., Vance, G.F., 1996. Sorption of the ionizable organic compound, dicamba (3,6-dichloro-2-methoxybenzoic acid), by organo-clays. *Chemosphere* 33 (10), 2089–2100.
- Chu, W., Wong, C., 2004. The photocatalytic degradation of dicamba in TiO<sub>2</sub> suspensions with the help of hydrogen peroxide by different near UV irradiations. *Water Res* 38 (4), 1037–1043.
- Chávez-Moreno, C., et al., 2013. On-line monitoring of the photocatalytic degradation of 2, 4-D and dicamba using a solid-phase extraction-multisyringe flow injection system. *J Environ Manag* 129, 377–383.
- Liu, J., et al., 2021. Enhanced degradation of dicamba by an anaerobic sludge acclimated from river sediment. *Sci Total Environ* 777, 145931.
- Gu, J.-G., Han, B., Duan, S., 2008. Initial transformation step of dicamba by a sulfate-reducing consortium enriched from sediment of the Pearl River of China. *Int Biodeterior Biodegrad* 62 (4), 455–459.
- Yao, L., et al., 2015. Degradation of the herbicide dicamba by two sphingomonads via different O-demethylation mechanisms. *Int Biodeterior Biodegrad* 104, 324–332.
- Li, X., et al., 2024. A review of metallurgical slags as catalysts in advanced oxidation processes for removal of refractory organic pollutants in wastewater. *J Environ Manag* 352, 120051.
- Liu, H., et al., 2023. Harnessing the power of natural minerals: a comprehensive review of their application as heterogeneous catalysts in advanced oxidation processes for organic pollutant degradation. *Chemosphere*, 139404.

- [15] Honarmandrad, Z., et al., 2023. Activated persulfate and peroxymonosulfate based advanced oxidation processes (AOPs) for antibiotics degradation—a review. *Water Resour Ind* 29, 100194.
- [16] Askarniya, Z., et al., 2022. A comparative study on the decolorization of Tartrazine, Ponceau 4R, and Coomassie Brilliant Blue using persulfate and hydrogen peroxide based advanced oxidation processes combined with hydrodynamic cavitation. *Chem Eng Process-Process Intensif* 181, 109160.
- [17] Askarniya, Z., Sadeghi, M.-T., Baradaran, S., 2020. Decolorization of Congo red via hydrodynamic cavitation in combination with Fenton's reagent. *Chem Eng Process-Process Intensif* 150, 107874.
- [18] Nan, H., et al., 2024. How does ball-milling elevate biochar as a value-added peroxydisulfate activator for antibiotics removal? *Ind Crops Prod* 214, 118569.
- [19] Askarniya, Z., et al., 2023. Degradation of bisphenol S—a contaminant of emerging concern—by synergistic ozone and percarbonate based AOP. *Water Resour Ind* 29, 100208.
- [20] Asadi, A.M.S., et al., 2024. Catalysts for advanced oxidation processes: deep eutectic solvents-assisted synthesis—A review. *Water Resour Ind* 31, 100251.
- [21] Yazdanbakhsh, A., et al., 2021. Dye degradation in aqueous solution by dithionite/UV-C advanced reduction process (ARP): Kinetic study, dechlorination, degradation pathway and mechanism. *J Photochem Photobiol A: Chem* 407, 112995.
- [22] Liu, X., et al., 2013. Photochemical degradation of vinyl chloride with an advanced reduction process (ARP)—effects of reagents and pH. *Chem Eng J* 215, 868–875.
- [23] Cichocki, L., et al., 2024. First highly effective non-catalytic nitrobenzene reduction in UV/dithionite system with aniline production—advanced reduction process (ARP) approach. *Chem Eng J* 479, 147878.
- [24] Liu, X., et al., 2016. Trichloroacetic acid reduction by an advanced reduction process based on carboxyl anion radical. *Chem Eng J* 303, 56–63.
- [25] Bao, Y., et al., 2018. Degradation of PFOA substitute: GenX (HFPO—DA ammonium salt): oxidation with UV/persulfate or reduction with UV/sulfite? *Environ Sci Technol* 52 (20), 11728–11734.
- [26] Vellanki, B.P., Batchelor, B., Abdel-Wahab, A., 2013. Advanced reduction processes: a new class of treatment processes. *Environ Eng Sci* 30 (5), 264–271.
- [27] Siefertmann, K.R., Abel, B., 2011. The hydrated electron: a seemingly familiar chemical and biological transient. *Angew Chem Int Ed* 50 (23), 5264–5272.
- [28] Liu, X., et al., 2015. Hydrated electron-based degradation of atenolol in aqueous solution. *Chem Eng J* 260, 740–748.
- [29] Schröder, D., et al., 1999. On the formation of the carbon dioxide anion radical  $\text{CO}_2^{\cdot-}$  in the gas phase. *Int J Mass Spectrom* 185, 25–35.
- [30] Liu, Y., et al., 2013. Enhancement of heterogeneous Cr(VI) reduction using clay minerals in the presence of organic carboxylic acids under UV irradiation. *Desalin Water Treat* 51 (37–39), 7194–7200.
- [31] Perissinotti, L.L., Brusa, M.A., Grela, M.A., 2001. Yield of carboxyl anion radicals in the photocatalytic degradation of formate over  $\text{TiO}_2$  particles. *Langmuir* 17 (26), 8422–8427.
- [32] Sun, S.-P., et al., 2009. Decolorization of an azo dye Orange G in aqueous solution by Fenton oxidation process: effect of system parameters and kinetic study. *J Hazard Mater* 161 (2–3), 1052–1057.
- [33] Flyunt, R., Schuchmann, M.N., von Sonntag, C., 2001. A common carbanion intermediate in the recombination and proton-catalysed disproportionation of the carboxyl radical anion,  $\text{CO}_2^{\cdot-}$ , in aqueous solution. *Chem—A Eur J* 7 (4), 796–799.
- [34] Tomanová, K., et al., 2017. At the crossroad of photochemistry and radiation chemistry: formation of hydroxyl radicals in diluted aqueous solutions exposed to ultraviolet radiation. *Phys Chem Chem Phys* 19 (43), 29402–29408.
- [35] Badmus, K., et al., 2016. Quantification of radicals generated in a sonicator. *Anal Bioanal Chem Res* 3 (1), 139–147.
- [36] Wang, M., et al., 2021. Spectrophotometric determination of hydrogen peroxide in water with peroxidase-catalyzed oxidation of potassium iodide and its applications to hydroxylamine-involved Fenton and Fenton-like systems. *Chemosphere* 270, 129448.
- [37] Capodaglio, A.G., 2020. Critical perspective on advanced treatment processes for water and wastewater: AOPs, ARPs, and AORPs. *Appl Sci* 10 (13), 4549.
- [38] Hendy, C.M., et al., 2021. Radical chain reduction via carbon dioxide radical anion ( $\text{CO}_2^{\cdot-}$ ). *J Am Chem Soc* 143 (24), 8987–8992.
- [39] Fedorov, K., Sun, X., Boczkaj, G., 2021. Combination of hydrodynamic cavitation and SR-AOPs for simultaneous degradation of BTEX in water. *Chem Eng J* 417, 128081.
- [40] Gu, X., et al., 2017. Carbon dioxide radical anion-based  $\text{UV}/\text{S}_2\text{O}_8^{2-}/\text{HCOOH}$  reductive process for carbon tetrachloride degradation in aqueous solution. *Sep Purif Technol* 172, 211–216.
- [41] Wang, J., Wang, S., 2021. Effect of inorganic anions on the performance of advanced oxidation processes for degradation of organic contaminants. *Chem Eng J* 411, 128392.
- [42] Huie, R.E., Clifton, C.L., Neta, P., 1991. Electron transfer reaction rates and equilibria of the carbonate and sulfate radical anions. *Int J Radiat Appl Instrum Part C Radiat Phys Chem* 38 (5), 477–481.
- [43] Wang, J., Wang, S., 2020. Reactive species in advanced oxidation processes: formation, identification and reaction mechanism. *Chem Eng J* 401, 126158.
- [44] Ghanbari, F., Moradi, M., Gohari, F., 2016. Degradation of 2,4,6-trichlorophenol in aqueous solutions using peroxymonosulfate/activated carbon/UV process via sulfate and hydroxyl radicals. *J Water Process Eng* 9, 22–28.
- [45] Ji, Y., et al., 2015. Heat-activated persulfate oxidation of atrazine: implications for remediation of groundwater contaminated by herbicides. *Chem Eng J* 263, 45–54.
- [46] Wang, J., Wang, S., 2018. Activation of persulfate (PS) and peroxymonosulfate (PMS) and application for the degradation of emerging contaminants. *Chem Eng J* 334, 1502–1517.
- [47] Fedorov, K., et al., 2020. Ultrasound-assisted heterogeneous activation of persulfate and peroxymonosulfate by asphaltenes for the degradation of BTEX in water. *J Hazard Mater* 397, 122804.
- [48] Rossi, R.A., 1982. Phenomenon of radical anion fragmentation in the course of aromatic SRN reactions. *Acc Chem Res* 15 (6), 164–170.
- [49] Costentin, C., et al., 1999. Thermal SRN1 reactions: how do they work? Novel evidence that the driving force controls the transition between stepwise and concerted mechanisms in dissociative electron transfers. *J Am Chem Soc* 121 (18), 4451–4460.
- [50] Rossi, R.A., Pierini, A.B., Peñéñory, A.B., 2003. Nucleophilic substitution reactions by electron transfer. *Chem Rev* 103 (1), 71–168.
- [51] Ding, C., et al., 2023. Environmental-friendly hydrochar-montmorillonite composite for efficient catalytic degradation of dicamba and alleviating its damage to crops. *Sci Total Environ* 856, 158917.
- [52] Gibb, C., et al., 2004. Remediating dicamba-contaminated water with zerovalent iron. *Chemosphere* 54 (7), 841–848.
- [53] Ghauch, A., 2001. Degradation of benomyl, picloram, and dicamba in a conical apparatus by zero-valent iron powder. *Chemosphere* 43 (8), 1109–1117.
- [54] Bianco-Prevot, A., et al., 2001. Continuous monitoring of photocatalytic treatments by flow injection. Degradation of dicamba in aqueous  $\text{TiO}_2$  dispersions. *Chemosphere* 44 (2), 249–255.
- [55] Li, D., et al., 2019. Synthesis of biomass tar-derived foams through spontaneous foaming for ultra-efficient herbicide removal from aqueous solution. *Sci Total Environ* 673, 110–119.
- [56] Huston, P.L., Pignatello, J.J., 1999. Degradation of selected pesticide active ingredients and commercial formulations in water by the photo-assisted Fenton reaction. *Water Res* 33 (5), 1238–1246.